Electronic Supplementary Material (ESI) for Journal of Materials Chemistry C.
This journal is © The Royal Society of Chemistry 2020

Supporting Information for

Tunneling-Induced Negative Permittivity in Ni/MnO Nanocomposites by a Bio-gel Derived Strategy

Peitao Xie,[1] Yifan Li,[2] Qing Hou,[3] Kunyan Sui,[1] Chunzhao Liu,*[1] Xueyan Fu,[2] Jiaoxia Zhang,[5]

Vignesh Murugadoss,[6,7] Jincheng Fan,[8] Yanpeng Wang,[9] Runhua Fan,*[4] Zhanhu Guo*[10]

[1] State Key Laboratory of Bio-fibers and Eco-textiles, Institute of Biochemical Engineering, College of Materials Science and Engineering, Qingdao University, Qingdao 266071, China

[2] Key Laboratory for Liquid-Solid Structural Evolution and Processing of Materials (Ministry of Education), Shandong University, Jinan 250061, China

[3] Kathleen Lonsdale Materials Chemistry, Department of Chemistry, University College London, 20 Gordon Street, London WC1H 0AJ, UK.

[4] College of Ocean Science and Engineering, Shanghai Maritime University, Shanghai 201306, China

[5] School of Materials Science and Engineering, Jiangsu University of Science and Technology, Zhenjiang 212003, China

[6]Key Laboratory of Materials Processing and Mold (Zhengzhou University), Ministry of Education, National Engineering Research Center for Advanced Polymer Processing Technology, Zhengzhou University, Zhengzhou, China

[7]School of Materials Science and Engineering, North University of China, Taiyuan 030051, China

[8] College of Materials Science and Engineering, Changsha University of Science and Technology, Changsha 410114, China

[9] College of Chemistry and Chemical Engineering, Henan University, Kaifeng 475004, China

[10] Integrated Composites Laboratory (ICL), Department of Chemical and Biomolecular Engineering, University of Tennessee, Knoxville, Tennessee 37996, United States

* E-mail: czliu@qdu.edu.cn (C. Liu); rhfan@shmtu.edu.cn (R. Fan); zguo10@utk.edu (Z. Guo).

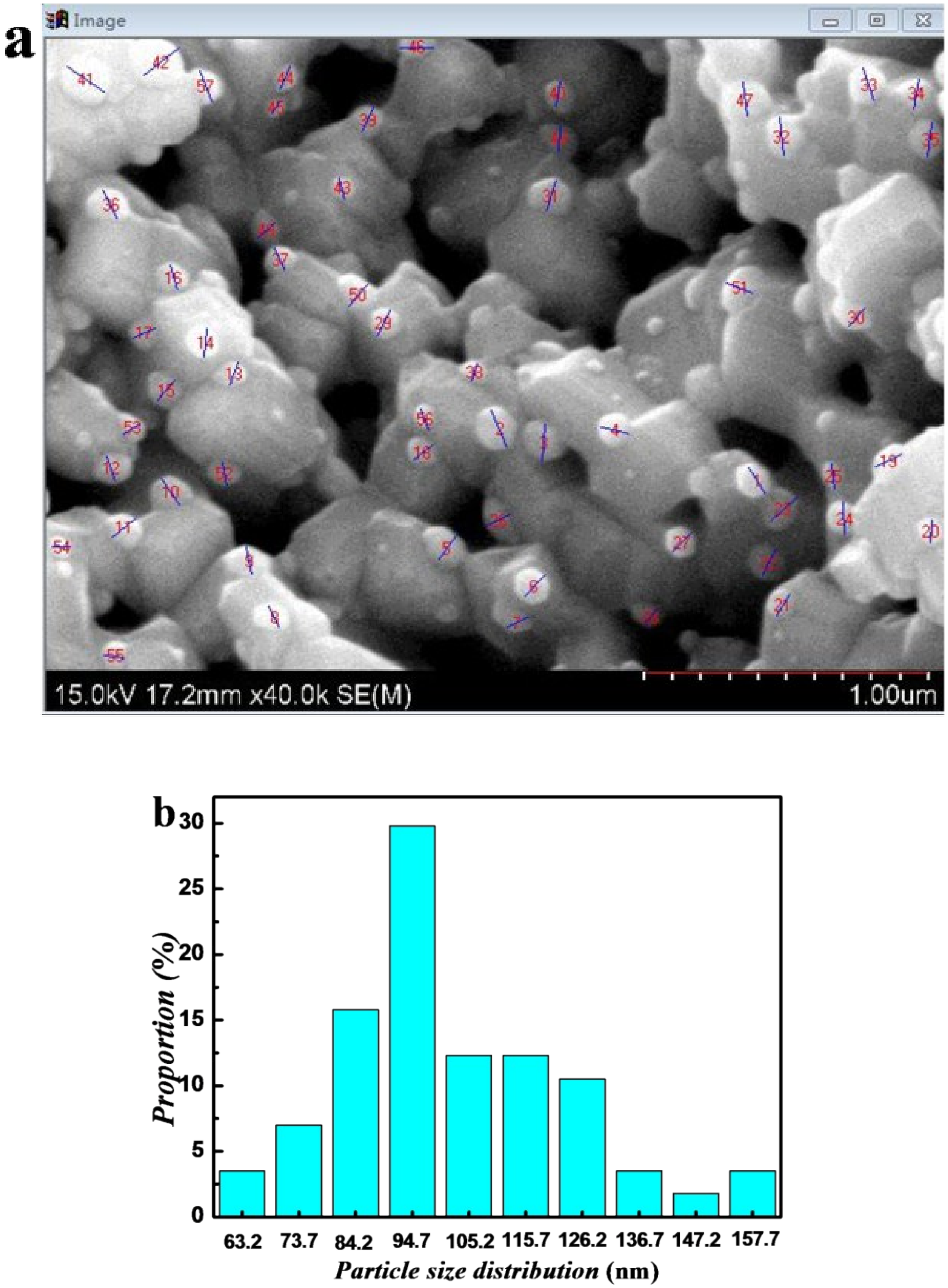

Fig. S1 (a) The SEM image used for particle size distribution, (b) the particle size distribution of Ni/MnO nanocomposites with Ni/Mn=20:80. The red number in (a) is serial number for nickel particle. There are 47 nickel particles considered for ensuring their size distribution.

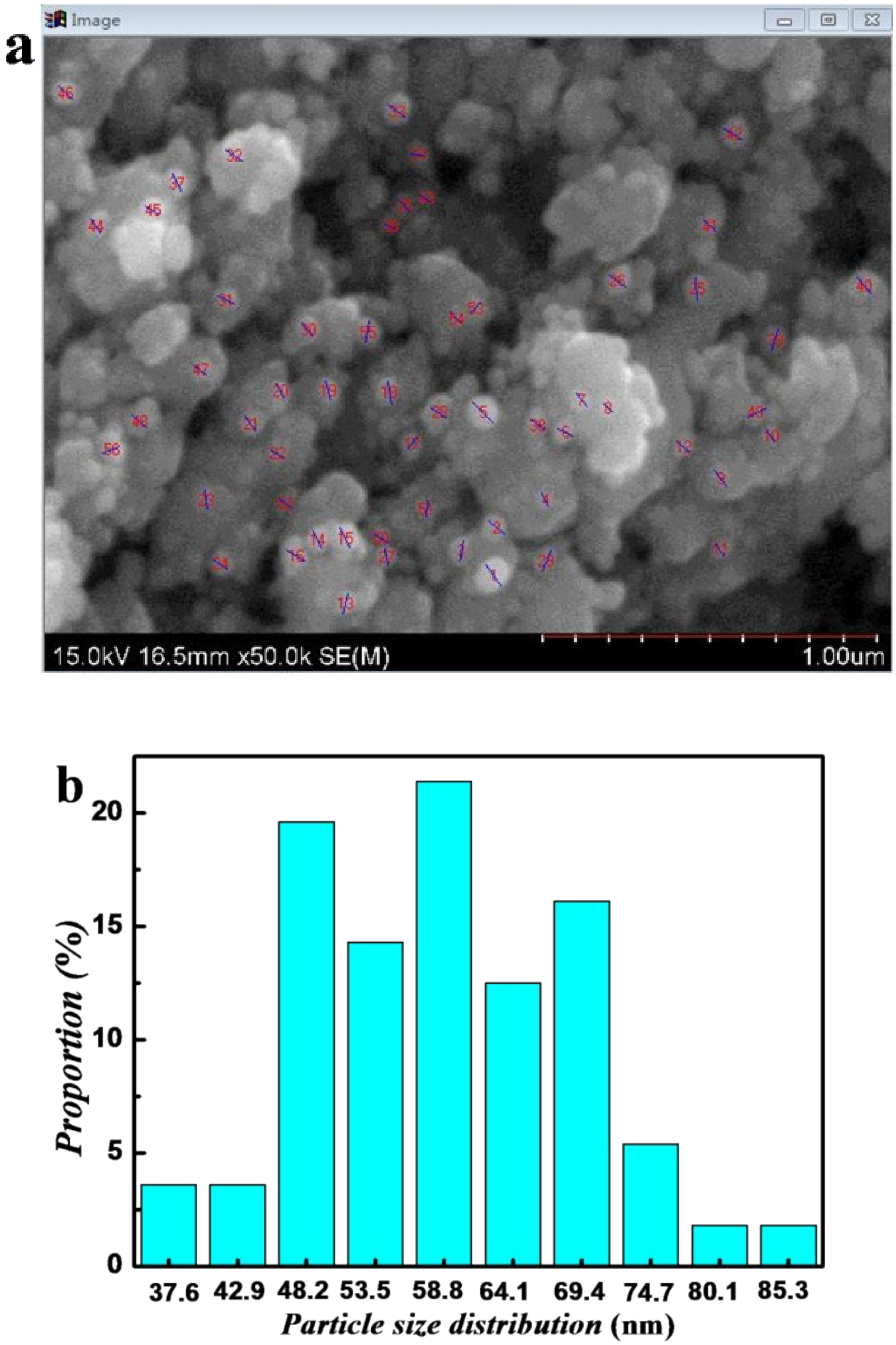

Fig. S2 (a) The SEM image used for particle size distribution, (b) the particle size distribution of Ni/MnO nanocomposites with Ni/Mn=40:60. The red number in (a) is serial number for nickel particle. There are 56 nickel particles considered for ensuring their size distribution.

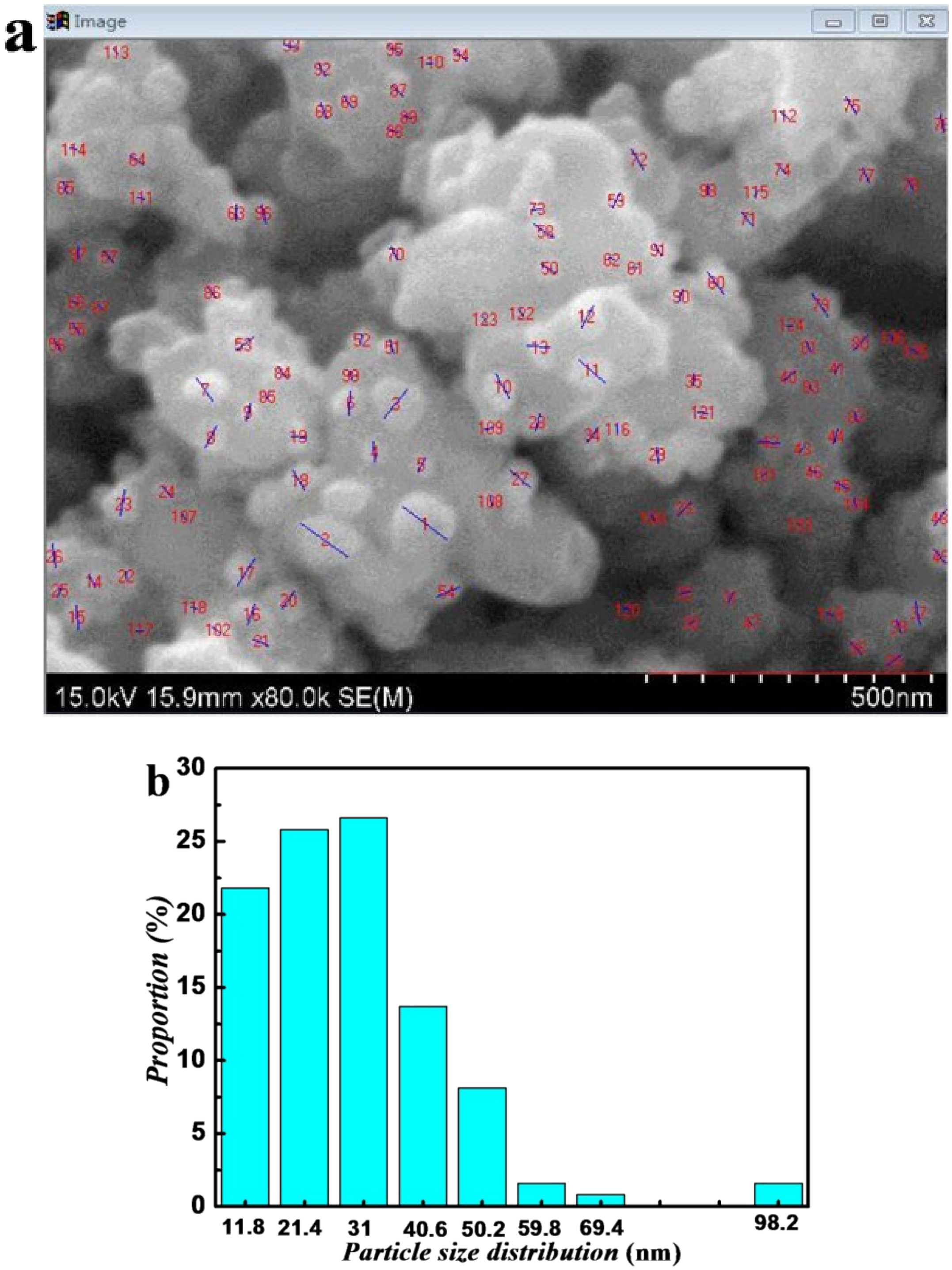

Fig. S3 (a) The SEM image used for particle size distribution, (b) the particle size distribution of Ni/MnO nanocomposites with Ni/Mn=60:40. The red number in (a) is serial number for nickel particle. There are 124 nickel particles considered for ensuring their size distribution.

The statistical data of nickel particle size are obtained by a Nano Measurer software in Ni/MnO nanocomposites of Ni/Mn=60:40. The total area of nickel particles in **Fig. S3a** is calculated by the following formula:

$$S = \sum_i \frac{\pi d_i^2}{4} \tag{S1}$$

where S is the sum of the area of all nickel particles in **Fig. S3a**, and d_i is the equivalent diameter of nickel particles. The value of S is 104574.64 nm^2, while the area of the SEM image is 1791521.49 nm^2. The nickel particles cover 5.84 % of the total area of the SEM images.

Table S1 Fitting parameters using the power law

	Fitting parameters		
Samples	***A***[a]	***n***[b]	**Reliability Factor**
MnO	5.912×10-14	1.4197	0.74635
Ni20	7.204×10-14	1.3122	0.95111
Ni40	5.603×10-12	1.1229	0.87236

[a] Apparent ahead parameter in power law. [b] exponential parameter in power law. The power law is in the form of $\sigma_{ac} = A\omega^n$.

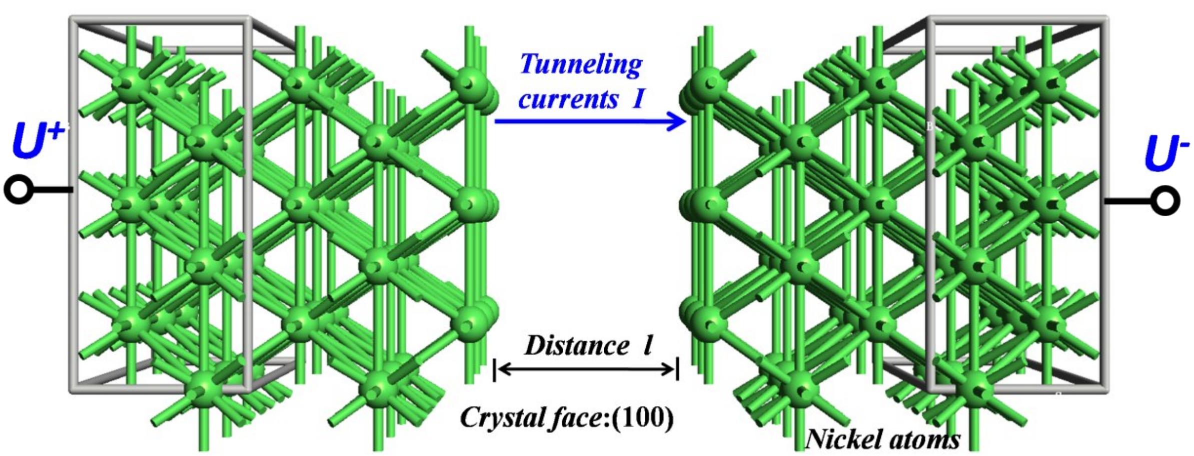

Fig. S4 Models of (100) crystal face to calculate tunneling conductivity using first-principles method.

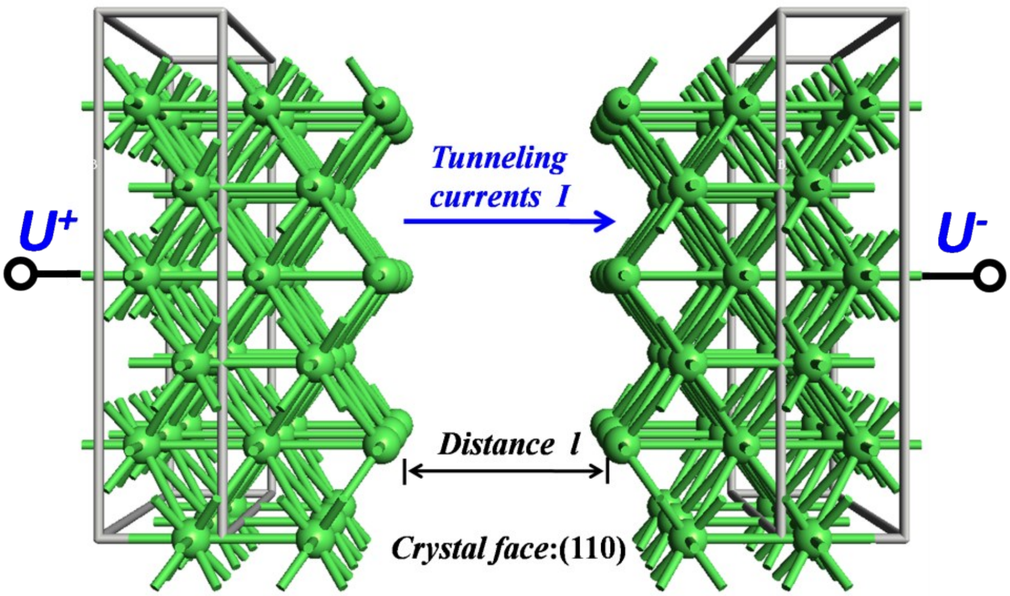

Fig. S5 Models of (110) crystal face to calculate tunneling conductivity using first-principles method.

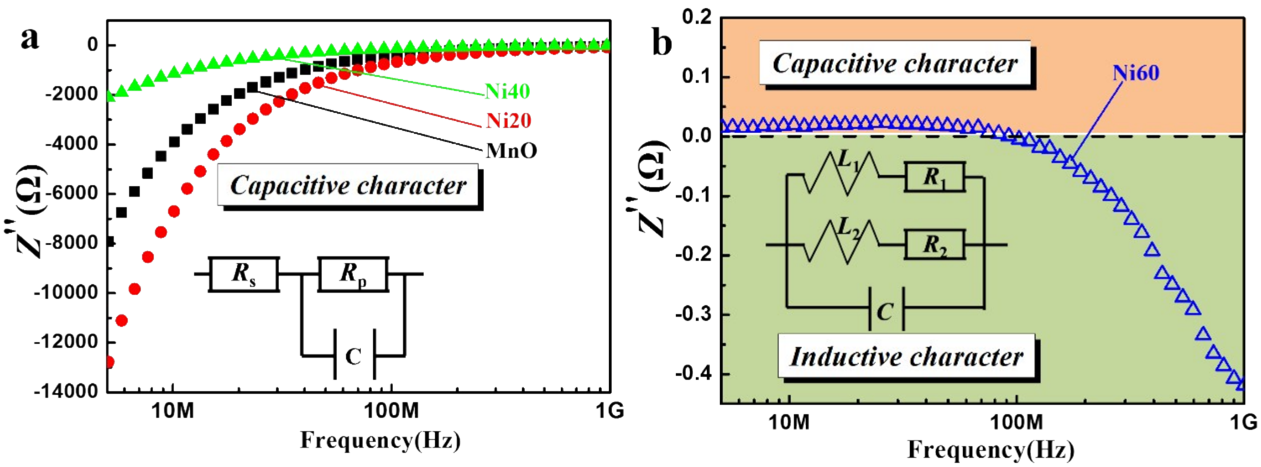

Fig. S6. The frequency dependence of reactance for Ni/MnO nanocomposites with different nickel content. The insets of (a) and (b) show equivalent circuits.

Equivalent circuit analysis was performed to further investigate the impedance spectra of nanocomposites. As shown in **Fig. S6a**, the reactance is negative, indicating capacitive behavior. The inset in **Fig. S6a** is their equivalent circuit by a series resistor R_s and a parallel connection of a resistor R_p and a capacitor C_p. The

R_s comes from the silver electrode, while the R_p results from the leakage current due to the mutual contact or agglometation of nickel particles.[S1] The reactance of Ni60 is positive at lower frequency range but turns to negative at higher frequency range (in the **Fig. S6b**). Interestingly, the positive-negative switching phenomenon for Z'' corresponded well to negative-positive switching for ε_r', indicating that negative permittivity behavior has inductive character while positive permittivity behavior has capacitive character.[S2] There are resistance R, inductance L and capacitance C in the equivalent circuits of Ni60 (in the inset of **Fig. S6b**). L is determined by tunneling current loops in the composites, while C is determined by the isolated nickel nanopartcles. As well known, the current of L would be decreased while the behavior of C is enhanced under the high-frequency external electric field, leading to the inductive–capacitive transitions with increasing frequency. Similar phenomena were also observed in Ag/YIG composites and $La_xSr_{1-x}MnO_3$ ceramics.[S3,S4]

As shown in **Fig. S7**, we built a square slab model (200 mm × 200 mm) with different thicknesses d (d = 0.1, 0.25, 0.5 and 1 mm), and perfect electric conductor (PEC) and perfect magnetic conductor (PMC) were used to simulate transverse electromagnetic wave (TEM) waveguide. The electromagnetic parameters of the Ni60 metacomposite in (**Fig. 7-9**) were used to conduct the electromagnetic stimulation. The scattering parameters (S11 and S12) were obtained, and shielding effectiveness (SE) was evaluated using **Equation S1-S5**. SE is the main evaluation criterion of suppressing electromagnetic interference (EMI). The SE total (SE_T) includes SE absorption (SE_A), and SE reflection (SE_R).

$$R = \left|S_{11}\right|^2 \tag{S1}$$

$$T = \left|S_{21}\right|^2 \tag{S2}$$

$$SE_R = -10\lg(1-R) \tag{S3}$$

$$SE_A = -10\lg\left[T/\left(1-R\right)\right] \tag{S4}$$

$$SE = SE_R + SE_A \tag{S5}$$

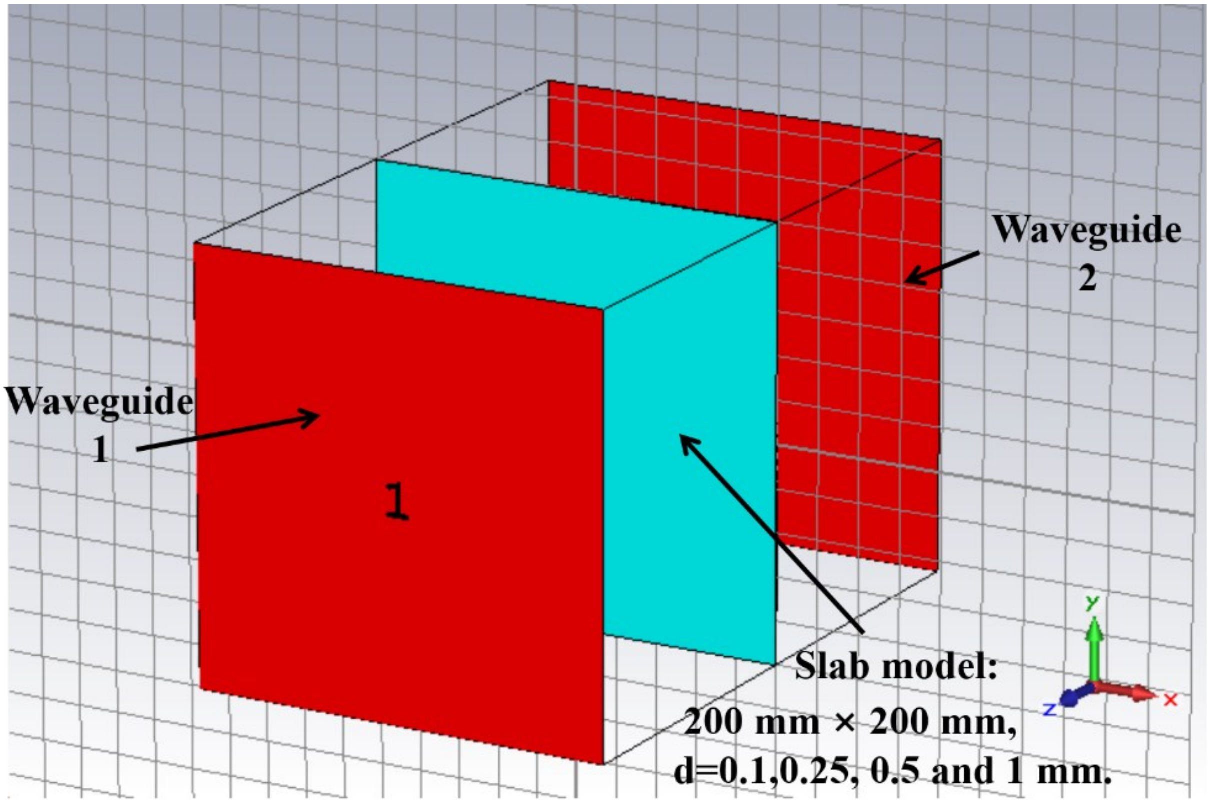

Fig.S7 The square slab model built for numerical simulation.

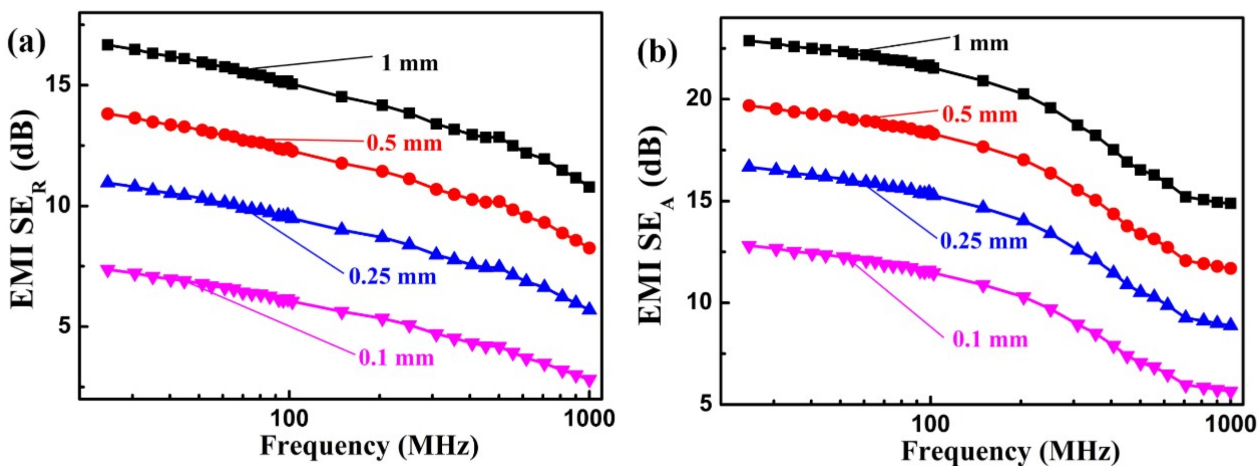

Fig. S8 Frequency dispersion of EMI SE_R (a) and SE_A (b) for Ni60 metacomposites with different thickness.

References

[S1] Z. Shi, R. Fan, Z. Zhang, H. Y. Gong, J. Ouyang, Y. Bai, X. Zhang, L. Yin, *Appl. Phys. Lett.*, 2011, 99(3): 032903.

[S2] P. Xie, K. Sun, Z. Wang, Y. Liu, R. Fan, Z. Zhang, G. Schumacher, *J. Alloy. Compd.*, 2017, 725, 1259-1263.

[S3] K. Sun, Z. Zhang, R. Fan, M. Chen, C. Cheng, Q. Hou, X. Zhang, Y. Liu, *RSC Adv.*, 2015, 5(75): 61155-61160.

[S4] K. Yan, R. Fan, Z. Shi, M. Chen, L. Qian, Y. Wei, K. Sun, J. Li, *J. Mater. Chem. C*, 2014, 2(6): 1028-1033.